Interband transitions, plasmons, and dispersion in hexagonal boron nitride

C. Tarrio and S. E. Schnatterly
Jesse W. Beams Laboratory of Physics, University of Virginia, Charlottesville, Virginia 22901
(Received 22 March 1989; revised manuscript received 26 May 1989)

We have measured inelastic-electron-scattering spectra of several hexagonal-boron-nitride samples with momentum transfer both in and out of the *a-b* plane and obtained the dielectric and optical constants from 0 to 60 eV. The low-q energy-loss spectrum with momentum in the plane is dominated by the π-electron plasmon at 8.5 eV and the total $(\sigma+\pi)$ plasmon at 26.4 eV. The π plasmon arises from two strong interband transitions at 6.1 and 6.95 eV, and a continuum threshold at 7.6 eV. The plasmons are well described as collective oscillations of bound electrons. We have inferred a band gap of 5.9 eV by observing the intrinsic absorption threshold in a series of samples of varying purity. The dispersion in the plasmons and the second interband transition is quadratic for $0<q<1.0$ Å^{-1}, while the first interband transition disperses upward in energy up to 0.6 Å^{-1}, above which its energy remains almost constant. The dispersion of the π plasmon is equal to that of the second interband transition, and its width remains constant up to a critical momentum, indicating that its width is dominated by decay into single-particle transitions. The energy-loss function with q along c shows three collective oscillations at 7.7, 11.7, and 23 eV. The interband spectrum is similar to that with q in the plane, except that an additional transition appears at 9.9 eV and the oscillator strength is shifted to higher energies. The similarity in the spectra for q in and out of the plane indicates nearly degenerate occupied σ and π states near E_F, which is inconsistent with existing band-structure calculations.

I. INTRODUCTION

In recent years, extensive experimental and theoretical attention has been devoted in hexagonal boron nitride (*h*-BN). First, BN is the lightest and most ionic of the III-V compounds, which are becoming increasingly important in the semiconductor device industry. Moreover, the allotropes of BN are isostructural to those of carbon, *h*-BN being isostructural to graphite. The electronic structure of *h*-BN also shares many similarities with graphite, although due to its ionicity and inequivalence of the lattice sites, *h*-BN is a wide-band-gap insulator, whereas graphite is a semimetal. Finally, *h*-BN is not well understood theoretically. While there is good agreement between various band-structure calculations and experiments for graphite, such is not the case for *h*-BN. The major reason for the conflicting experimental results is the inavailability of large pure samples. While large pure crystals of highly ordered pyrolytic graphite are commercially available, the mismatch in the sizes of the B and N ions make the production of large single crystals impossible with present sample preparation methods, leading to great variation in the electronic properties from sample to sample.

At the heart of the confusion over the electronic properties of *h*-BN is a reliable value for the band gap. This confusion arises from measurable impurity states below the intrinsic gap whose optical absorption begins as low as 1 eV.[1] Previous electron energy-loss results report a band gap of 5.7 eV,[2] while optical-absorption groups report 3.8 (Ref. 3) to 5.8 eV (Ref. 4), and reflectivity measurements find 5.2 eV (Ref. 5). Band-structure calculations have reported values of 2.45 (Ref. 6) to 12.7 eV (Ref. 7) with most reporting direct gaps,[6–12] but Ref. 13 reporting an indirect band gap of 3.9 eV and a direct gap of 4.3 eV. The band structures calculated for *h*-BN are very sensitive to the method of calculation. Zunger[11] finds that results depend strongly on the cluster size when using a truncated–molecular-cluster approach, while Zunger, Katzir, and Halperin[8] find band gaps varying from 3.7 to 5.5 eV using three different Hückel techniques. Nakhmanson and Smirnoff[6] report that the calculated band gap increases from 2.45 to 3.8 eV upon increasing the number of augmented plane waves from 73 to 150 in their study, and Catellani *et al.*[13] point out the importance of reaching self-consistency.

In the present investigation, we have measured inelastic-electron-scattering (IES) spectra of three *h*-BN samples from 0 to 60 eV with momentum transfer in the *a-b* plane. The samples were of varying purity, with the signal in the band-gap region varying by a factor of 4. Via a Kramers-Kronig (KK) analysis we obtain the dielectric and optical constants. We study the origins of the plasmons in terms of electron densities and their positions relative to other excitations. By measuring characteristics of samples of varying purity, we are able to observe a sharp absorption threshold common to all three samples, which we conclude is the intrinsic band gap. In light of the extreme differences in the electronic properties of *h*-BN properties reported in the literature, we discuss the similarities and differences found in our samples. We have also measured spectra of samples with momentum transfer at angles out of the *a-b* plane. From these measurements we obtain the optical constants of *h*-BN with momentum transfer along the *c* axis. These results coupled with the results for q in the *a-b* plane provide ad-

ditional insight into the band structure of h-BN. We also provide evidence for an additional longitudinal collective electronic excitation.

II. DATA ACQUISITION AND ANALYSIS

Samples of pyrolytic BN were cleaved with adhesive tape and separated from the tape with chloroform. The flakes were then ultrasonically cleaned with a series of organic solvents and finally etched in a HF-H_2SO_4-H_2O_2-H_2O solution.[14] The clean samples were then mounted with vacuum-compatible epoxy onto stainless-steel sample holders and some were argon-ion milled. The milling voltage was initially 5 kV, and was decreased gradually to 500 V over several hours after pinholes were noticed, to reduce surface damage in the samples. Samples from three batches of varying purity were used for the measurements with q in the a-b plane. Sample 1 was of a brownish color, indicating a high density of defects, while samples 2 and 3 appeared whitish, indicating fewer impurities. Transmission measurements were made on the Virginia inelastic-electron-scattering accelerator, which has been described in Ref. 15. The primary beam energy was 290 keV, with energy resolution of 0.18 eV and momentum resolution between 0.04 and 0.06 Å^{-1}. Measurements were taken at constant values of transverse momentum transfer between 0.13 and 1.0 Å^{-1}.

Figure 1 shows low-q energy-loss functions for the three samples. The IES cross section is

$$\frac{d^2\sigma}{d\omega\, d\Omega}=\frac{8\pi e^2}{\hbar q^2}\,\mathrm{Im}\left[-\frac{1}{\epsilon(q,\omega)}\right],$$

where q is the momentum transfer and ϵ the complex dielectric function. To obtain the final energy-loss functions, $\mathrm{Im}[-1/\epsilon(q,\omega)]$, the spectra must be corrected for multiple-scattering events, in which one fast electron scatters off more than one excitation, and kinematic effects, which arise from the energy dependence of the $1/q^2$ weighting factor. These corrections are made following algorithms of Fields[16] and Livins and Schnatterly.[17] The amount of multiple scattering removed and the final scale of the spectra are determined by satisfying both $\epsilon_1(\omega=0)=4.9$ (Ref. 18) for q in the a-b plane and the oscillator strength sum rule assuming $N_{\mathrm{eff}}(\omega\rightarrow\infty)=8.5$ electrons. We arrive at the value of 8.5 electrons because the spectra are truncated at an energy below both the B and N 1s core levels, leaving 8 electrons per formula unit. We graft on a $1/\omega^3$ tail above 60 eV to extrapolate to $\omega\rightarrow\infty$. The extra 0.5 electron arises from the fact that lower-energy excitations generally carry more oscillator strength than the actual number of electrons per formula unit due to the negative oscillator strength for transitions into lower-energy states.[19]

A KK analysis allows us to determine $\mathrm{Re}[\epsilon(q,\omega)]^{-1}$,

$$\mathrm{Re}\left[\frac{1}{\epsilon(q,\omega)}\right]-1=\int_0^\infty \frac{1}{\omega'^2-\omega^2}\,\mathrm{Im}\left[\frac{1}{\epsilon(q,\omega')}\right]d\omega',$$

and also the dielectric and optical constants. Figure 2 shows the dielectric constants, ϵ_1 and ϵ_2, obtained from a KK analysis of the data for sample 3 in Fig. 1. The ϵ_1 spectrum shows upward zero crossings at 8.2 and 24.8 eV, indicating that the peaks at 8.6 and 26.4 eV in the loss function are plasmons. The partial plasmon at 8.6 eV arises from the collective oscillation of the π electrons, while the peak at 26.4 eV is the total plasmon, arising from oscillations of the $\sigma+\pi$ electrons. The ϵ_1 spectra for some q values exhibit upward zero crossings at 6.8 eV, leading to the shoulder in the loss functions. The reason that all spectra do not have zero crossings at this energy is due to the uncertainty in the counting statistics, which leads to larger uncertainties in the KK analyses. The low-q ϵ_2 spectra show strong transitions at 6.1, 6.95, and 14.7 eV. In a previous IES study, Büchner[2] reports low-q peaks at approximately the same energies, though

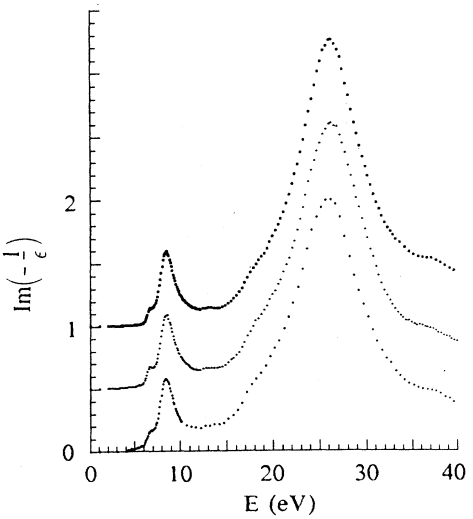

FIG. 1. Energy-loss functions for three h-BN samples, top to bottom: sample 3, sample 2, and sample 1.

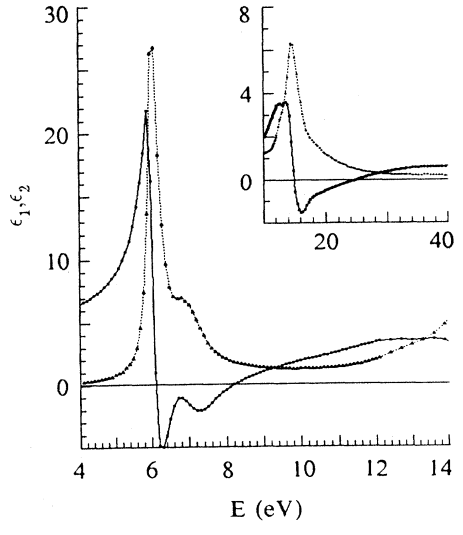

FIG. 2. Dielectric constants for sample 3, $q=0.13$ Å^{-1}: solid line, squares, ϵ_1; dotted line, triangles, ϵ_2.

due to lower energy resolution, his low-q peaks are broader, and thus are reduced in amplitude.

To obtain optical constants for q along c, we have measured spectra of samples mounted with the c axis 15°, 30°, and 45° from the incident beam. Spectra were measured at $q=0.15$ Å^{-1} transverse momentum transfer. At low energies and momentum transfers, it is a good approximation to assume that the momentum transfer is perpendicular to the incident beam. In this limit, the dielectric constants for a sample mounted with the c axis at an angle θ to the incident beam take the form[20]

$$\epsilon(q,\omega,\theta)=\epsilon_{\parallel}(q,\omega)\sin^2\theta+\epsilon_{\perp}(q,\omega)\cos^2\theta ,$$

where $\epsilon_{\perp}$ is the dielectric constant in the a-b plane and $\epsilon_{\parallel}$ is the dielectric constant with q parallel to the c axis. To obtain the parallel dielectric constants, we evaluate the loss functions measured at angle θ as described above, assuming 8.5 electrons and $\epsilon_{1\perp}(\omega\rightarrow 0)=4.9$ and $\epsilon_{1\parallel}(\omega\rightarrow 0)=4.1$.[18] The appropriate amount of the known spectrum with q in the plane is then subtracted and the resultant spectrum is rescaled for 8.5 electrons and $\epsilon_{1\parallel}(\omega\rightarrow 0)=4.1$.

III. DISCUSSION

A. Momentum transfer in the a-b plane

The three samples measured show varying signal in the band-gap region. Absorption begins between 2 and 3 eV in samples 2 and 3, and at 3 to 4 eV in sample 1. The amplitude of the loss function at 5 eV is smallest in sample 3. The amplitude at 5 eV in sample 2 is roughly double that of sample 3, and in sample 1, about four times that of sample 3. Although the gap signal of insulators often takes the form of Gaussian peaks due to color centers, in these measurements the signal in the gap region is well described by a straight line. This behavior has also been observed by Hoffman, Doll, and Eklund.[1] Assuming slowly varying matrix elements, this shape arises from the joint density of states between the occupied states near the Fermi level and the vacant states present due to defects. The density of occupied states show a sharp downward slope near E_F,[13] therefore the density of band-gap states must be sharply sloped upward to show the linear behavior we observe. Figure 3 shows the result of fitting a straight line from 2 to 5 eV to spectra of sample 3 obtained at 0.13 and 1.0 Å^{-1}, and subtracting these contributions from the spectrum. The intrinsic energy gap occurs at 5.8 eV in both cases, indicating a direct gap.

The greatest consequence of the varying sample quality occurs in the Kramers-Kronig analysis. The extrapolation to zero energy and the scaling of the spectrum to satisfy $\epsilon_1(0)=4.9$ (Ref. 18) depend strongly on both the shape and magnitude of the spectrum at low energy. Generally, the sharper the intrinsic threshold, or the weaker the band-gap signal, the greater the amplitude of the first peak in ϵ_2. Thus, the 6-eV peak in ϵ_2 in sample 3 has a height of 28, while in samples 2 and 1, the heights are 22 and 18, respectively. Since sample 3 is the purest of three samples studied, its properties are presumably

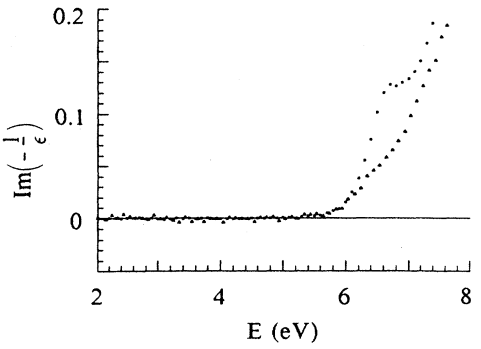

FIG. 3. Energy-loss functions for sample 3 with linear background subtraction of band-gap signal: squares, $q=0.13$ Å^{-1}; triangles, $q=1.0$ Å.

closest to intrinsic, and we will concentrate most of the discussion on its properties, summarizing the parameters of all three samples for comparison.

Figure 4 shows final loss functions for a range of q values between 0.13 and 1.0 Å^{-1}. The plasmon positions are described well in terms of collective oscillations of bound electrons. One expects plasma frequencies to shift upward due to excitations below the plasma frequency, and downward due to excitations higher in energy. In BN, both occur. The shift in the energy can be described approximately by[20]

$$\omega_p'^2=\frac{\omega_{p0}^2+\omega_n^2}{1+\chi_b} ,$$

where $\omega_{p0}^2=4\pi ne^2/m$ is the "bare" plasma frequency in the absence of other excitations, ω_n is an eigenfrequency of the electrons participarting in the collective oscillation, and χ_b is the polarizability of the electrons lying in more deeply bound shells. We take ω_n to be the energy

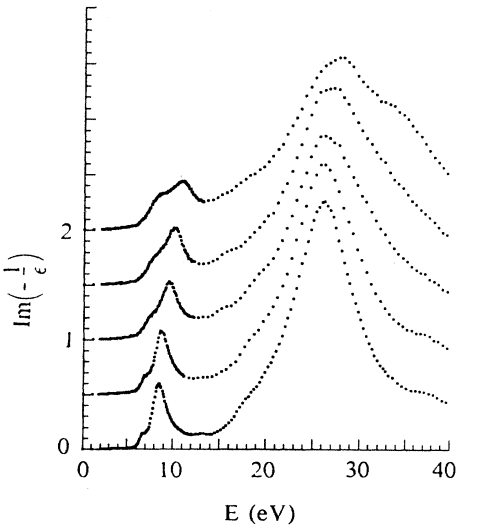

FIG. 4. Energy-loss functions for sample 3, bottom to top: $q=0.13$, 0.31, 0.55, 0.80, and 1.00 Å^{-1}.

of the largest peak in ϵ_2. From the electron density, we find $\hbar\omega_{p0}=12.3$ eV for the π plasmon, and 24.6 eV for the total plasmon. Taking $\hbar\omega_n=6.1$ eV for the π band and 14.6 eV for the σ bands, we obtain plasma frequencies of 8.5 and 26.4 eV with background polarizabilities of 1.7 above the π plasmon and 0.1 above the σ plasmon. These values compare favorably with other sets of electrons lying at similar energies. The total plasmon shape near its peak is well described by a Drude shape, which can be expected when the plasmon energy is much larger than the band gap, and the plasmon lies well away from other excitations. Although the N 2*s* electrons are active below 20 and above 30 eV, in the range 20–30 eV, their contribution has little shape. Drude fits to the shape in this energy region yield a zero-q plasma energy of 26.4 eV, and a half-width of 8.4 eV.

The shape in the region of the π peak is somewhat more complicated. The π peak lies above another peak at 6.8 eV, and an error-function-like threshold which appears at 7.7 eV. This threshold has an amplitude of about 0.35 and leads to the asymmetry in the π plasmon and the flatness in the region above 10 eV. We have fit the spectra in this region with two Lorentzians and an error function, yielding an energy an energy of 6.8 eV for the first excitation and a plasma frequency of 8.65 eV with a width of 1.7 eV. Surprisingly, we find no dispersion in the width of the π plasmon at momentum transfers below 0.8 Å^{-1}. One may expect that, since the π plasmon is lying on a continuum of excitations, its width even at low q will be dominated by decay into single-particle excitations. This will lead to a lack of dispersion in the width of the plasmon as we have observed.

The ϵ_2 spectra are also described well in terms of two Lorentz oscillators and a continuum threshold. It was found that this continuum threshold took the square-root shape expected above a critical point in the joint density of states.[21] The threshold appears at about 7.6 eV and does not disperse with momentum. Presumably, this threshold arises from the same excitations as the 7.7-eV threshold in the loss function, and though it is difficult to see due to the intensity of the interband transitions, it presence is essential to describe the shapes of the spectra in this energy region. ϵ_2 spectra and fits are shown in Fig. 5. The peaks we measure at 6.1 and 6.95 eV are predicted by band structure[12–14] to originate from transitions near the *L-M* axis of the Brillouin zone between nearly degenerate bands. Doni and Parravicini[12] predict energies of 6.2 and 6.9 eV, very close to our $q=0$ values of 6.1 and 6.95 eV. Catellani *et al.*,[13] likewise, find a doublet peak centered around 6.5 eV. Robertson[9] places the π valence bands at *M* 2 eV below E_F, thus overestimating the transition energy. Our measured dispersions of these transitions are shown in the bottom two lines in Fig. 6. The higher-energy transition disperses quadratically at 2.4 eV Å^2, while the lower-energy peak disperses at 0.7 eV Å^2 out to 0.6 Å^{-1}, and remains constant at higher momentum transfers. For sharp transitions, the dispersion arises from the curvatures of the bands and is proportional to $1/m_e+m_h$. Thus, the dispersion will be small if either the electron or hole mass is very large. We have not found any band-structure calculations which can account for the small dispersion in the first interband peak.

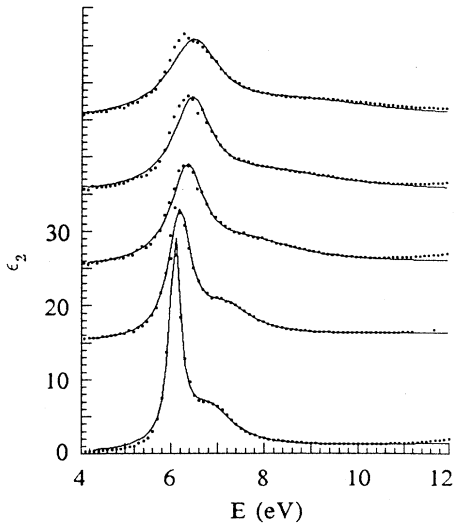

FIG. 5. ϵ_2 spectra (squares) with fits (lines) consisting of two Lorentz oscillators with a square-root threshold, from bottom to top: $q=0.13$, 0.31, 0.55, 0.80, and 1.00 Å^{-1}.

The widths of the peaks also disperse somewhat. The width of the 6.95-eV peak disperses at roughly the same rate as the energy (3.0 eV Å^2). However, the width of the first peak disperses at 1.0 eV Å^2, and it continues to broaden above 0.6 Å^{-1}. This is most likely due to averaging over more than one crystal direction. Under an optical microscope, we can observe mosiac patterns in our samples, indicating that crystallites may lie with their *a* axes not uniformly aligned. The transition energies are

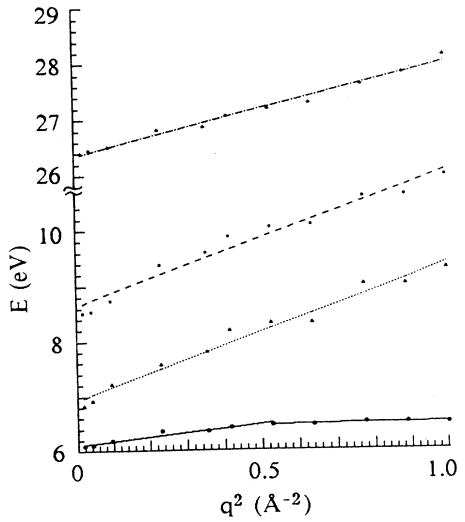

FIG. 6. Sample 3 peak dispersion for first two interband peaks and plasmons.

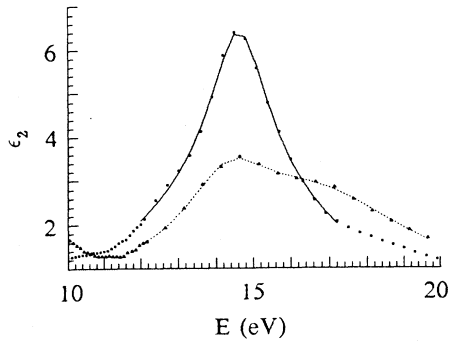

FIG. 7. ϵ_2 spectra in the σ-σ transition region: squares, solid line, $q=0.13$ Å^{-1}; triangles, dotted line, $q=0.8$ Å^{-1}.

predicted to be almost identical at the M and L points.[12,13] Thus if the one peak actually arises from two transitions nearly degenerate in energy at low q and the band disperses differently along the $L-A$ axis than along the $M-L$ axis, we will observe a single peak which broadens faster than it shifts up in energy. Furthermore, we notice a growing asymmetry in the first peak as we move out in momentum as shown in the fits in Fig. 5. This, likewise, is most likely due to two transitions which are degenerate at low q, but which disperse at different rates along different axes. We have tried generating these shapes by adding extra peaks without success.

The origin of the thresholds at 7.6 in ϵ_2 and 7.7 eV in $\mathrm{Im}(-1/\epsilon)$ is ambiguous. Band structure indicates σ-σ band gaps of 6.0 (Refs. 1 and 13) to 10.0 eV,[8,9] so the onset of σ transitions may occur at 7.6 eV. Additional information may be gathered from angle-resolved core spectroscopy experiments which are able to distinguish between σ and π states. From soft-x-ray emission[22,23] (SXE) and x-ray photoemission (XPS),[24] it has been determined that the tail of the occupied σ density of states extends almost up to the Fermi level, and increases sharply with decreasing energy about 2 eV below E_F. The σ threshold in an angle-resolved IES measurement[25] of the B K edge occurs about 3–5 eV above the π threshold, depending on the π-exciton binding energy. The oscillator strength sum rule also yields more information. At low q, the first two peaks in ϵ_2 each contain about 0.65 electrons of integrated oscillator strength, giving a total of only 65% of the expected two π electrons. However, the peaks grow in strength with increasing q, while the threshold at 7.6 eV loses strength, until the peaks saturate at 2.4 electrons, and the threshold has virtually disappeared. Since the redistribution of strength is continuous and gradual, the threshold at 7.6 eV most likely contains π electrons. As this threshold loses strength, another threshold at 11.0 eV behaves fairly consistently (notice the deviation from the fits in Fig. 5), and we conclude that the threshold at 11.0 eV is the onset of σ-σ transitions. This is consistent with other experiments,[22–25] assuming that occupied σ bands extend almost up to E_F and the unfilled σ states begin 5 eV above the lowest unoccupied π levels.

The 14.7-eV peak is also a doublet. The spectra were fit with two Lorentzians and a constant background. At low q, the two peaks are degenerate, with a splitting smaller than the uncertainty. Although the precise dispersion is quite uncertain, the one peak disperses downward in energy slightly, while the other disperses upward. The lower-energy peak retains its width of 3.5–4.5 eV while dispersing from 14.7 down to 14.2 eV. Meanwhile, the other peak increases in energy from 14.7 at 0.13 Å^{-1} to 17.2 eV at 0.8 Å^{-1}, as shown in Fig. 7, while also increasing in width from 4.5 to 8 eV, making precise determination of energies impossible at higher q values. This anomalous dispersion arises from two bands degenerate at a symmetry point which are split as the transitions become nonvertical further out in momentum. These results are in agreement with transitions near the $A-\Gamma$ axis in Robertson's calculations,[9] however, other calculations predict lower energies for these transitions.[12,13]

Band-structure calculations indicate a band of mostly N 2s character 16 (Ref. 11) to 19 eV (Refs. 5, 12, and 13) below the lowest unoccupied level. SXE (Refs. 22 and 23) and XPS,[24] meanwhile, indicate a binding energy of 15 eV below E_F. We attribute the shoulder in the loss function at about 18 eV to the N 2s threshold. We do not expect this threshold to have any sharp structure due to the width of the level and the mixed character of the unoccupied states.

One of the more important aspects of this work is the study of the variation between the properties of the different samples. As expected in light of the discrepancies in the properties of h-BN reported in the literature, we have seen some variation in most of our measured parameters. Energies and dispersion parameters are summarized in Table I. As pointed out earlier, any absorption in the band-gap region will affect the KK analysis dramatically, and other properties are affected, too. The band gap of each spectrum measured on each sample was evaluated by subtracting a linear signal fit from 2 to 5 eV, and the averages for samples 1 and 2 were 5.9 eV, while that for sample 3 was 5.8 eV. The minimum value observed was 5.7 eV, and the maximum, 6.1 eV, so we may conclude that these samples have a band gap of 5.9±0.2 eV. In all cases, the scatter in the values was random

TABLE I. Energies (E_i, eV) and dispersions (m_i, eV Å^2) of interband transitions and plasmons and band gaps (E_g, eV) for the three samples studied.

Sample	E_1	m_1	E_2	m_2	E_π	m_π	$E_{\sigma+\pi}$	$m_{\sigma+\pi}$	E_g
1	6.01	0.74	6.91	3.3	8.41	3.42	26.3	2.0	5.9
2	6.10	0.71	6.97	3.1	8.52	3.12	26.6	1.4	5.9
3	6.10	0.71	6.93	2.4	8.65	2.42	26.4	1.6	5.8

rather than decreasing with q, so the gap is direct within uncertainty. A small increase in the gap signal was observed for some spectra, however, this is most likely due to radiation damage, as it is correlated with electron beam dose on the sample rather than with higher-q spectra. The zero-q energies and the dispersions of the plasmons and interband transitions were found by fitting straight lines to the calculated peak positions versus q^2. The energies of the zero-q interband transitions vary by less than 0.1 eV, and the thresholds at 7.6 and 11.0 eV in ϵ_2 by a few tenths of an eV, although they are much harder to determine. The second interband transition and the π plasmon, however, disperse much less in sample 3 than in the other two. The origin of this discrepancy is not clear and requires further study. In all three samples, the dispersion of the π plasmon is parallel to the second interband transition. This is consistent with the model of the longitudinal excitation lying slightly higher in energy than a corresponding transverse excitation.[19] The spread in the plasma frequencies was 0.2 eV for the π plasmon and 0.3 eV for the σ plasmon. This can be expected, since none of the crystals are perfect, and therefore, their densities probably differ somewhat.

B. Momentum transfer along the c axis

In hexagonal compounds, selection rules for electronic transitions depend on whether momentum transfer is parallel or perpendicular to the a-b plane. In fact, with q in the plane, only transitions between bands of the same parity are allowed (π-π and σ-σ), while with q parallel to c, only transitions between bands of different parity are allowed (π-σ and σ-π).[26] Chen and Silcox[27] have shown that relativistic effects make a significant contribution to the IES spectra of graphite. However, the excitations arising from these effects disappear at momentum transfers between 0.01 and 0.03 Å^{-1}. In our experiments, with resolution of 0.06 Å^{-1} and momentum transfer of 0.15 Å^{-1}, excitations at momenta less than 0.03 Å^{-1} contribute less than 10^{-6} of our signal, and are therefore inconsequential. Additionally, relativistic effects can cause transverse character in the excitations created by the electron beam. These contributions were evaluated using standard electrodynamics[28] and found to be insignificant (on the order of 10^{-9}). Anisotropic dielectric constants have been studied extensively in graphite.[26–32] In addition to the angle-resolved core spectroscopy,[22–25] angle- and polarization-dependent reflectivity has been measured on h-BN between 5 and 30 eV.[33] The loss function and dielectric constants we have obtained for q along c are shown in Figs. 8 and 9.

The qualitative differences between our measured parallel and perpendicular spectra are similar to those found in graphite.[26,29–32] The $\pi+\sigma$ plasmon has shifted down from 26.4 to 23 eV. Many *et al.* found a shift of 27 to 21 eV,[31] while in graphite the reported shift has been from 37 to 20 eV.[30–32] Meanwhile, it is not clear in our spectra whether the π plasmon has shifted down to 7.7 or up to 11.7 eV. Peaks appear in the loss function at those energies, and ϵ_1 shows a minimum at 7 eV and an upward zero crossing at 11 eV, both where ϵ_2 is small. This is

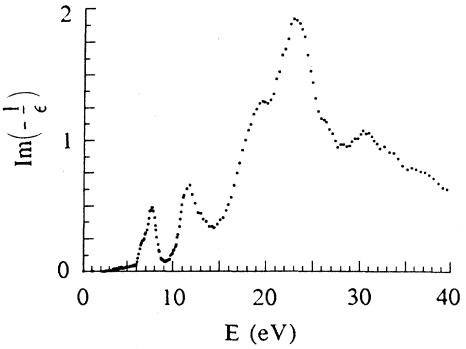

FIG. 8. Loss function with q along the c axis.

strong evidence that either or both of the peaks in the loss function are plasmons. Correspondingly, graphite with q along c shows sharp peaks in the loss function at 5.3 and 20 eV, a minimum in ϵ_1 at 5 eV and zero crossings in ϵ_1 at 14 and 19 eV.[26,21,32] At 14 eV there is not a sharp peak in the loss function, rather there is a shoulder. However, the 5-eV loss peak does not show a zero crossing in ϵ_1, leading Tosatti and Bassani[26] to conclude that the shoulder in graphite at 15 eV is the π plasmon. In the case of BN, both the 7.7- and 11.7-eV peaks lie near minima of ϵ_2, eliminating the possibility that they arise from strong interband peaks. We must therefore conclude that three peaks, at 7.7, 11.7, and 23 eV, arise from collective longitudinal oscillations.

Surprisingly, the interband transitions are quite similar to the case with q in the a-b plane. The peaks at 6.10, 6.85, and 14.9 eV with q along c look very much like the peaks at 6.10, 6.95, and 14.7 eV with q in the a-b plane, except that the strengths are somewhat reduced. The first doublet contains only 0.9 electrons, compared to the 1.3 electrons with q along c. An additional strong peak is present at 9.9 eV, and the peak at 14.9 eV has shifted up

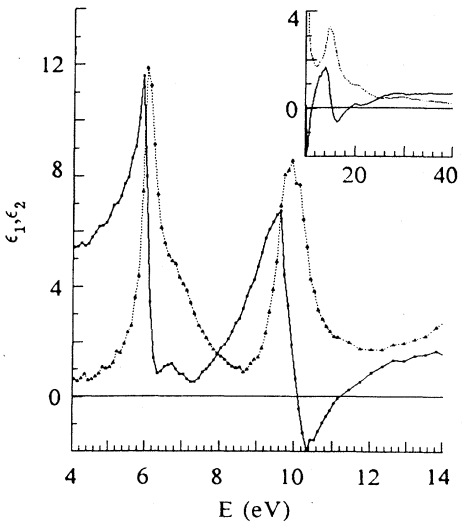

FIG. 9. Dielectric constants with q along c: solid line, squares, ϵ_1; dotted line, triangles, ϵ_2.

0.2 eV in energy and lost amplitude. Additional structure is also present at 20 and 30 eV. Both the additional interband peak and the added oscillator strength above 20 eV are similar to the changes in graphite.[26]

Existing band-structure calculations cannot explain the low-energy peaks in the ϵ_2 spectrum. Since the lowest unoccupied σ bands lie well above the unoccupied π bands,[25] and the occupied σ bands extended almost up to E_F,[22-24] the low-energy part of the spectrum with q along the c axis must consist of transitions from filled σ bands into empty π bands. The lowest direct σ-π transitions are predicted to be 8.4 eV (Ref. 13) to 12.2 eV.[9] Moreover, due to the overall similarity in the low-energy transitions (energy and width), they appear to involve the same final states with q in or out of the a-b plane. Thus, the transitions must occur near the $L-M$ axis, and the initial π and σ states must be nearly degenerate in energy. This point is reinforced by the similarity between the σ-σ peak at 14.7 eV and the π-σ peak at 14.9 eV. A difference of 0.2 eV at that energy can easily occur due to uncertainties in the KK analysis coupled with the fact the peak is very broad. This also appears to be a transition into the same state from nearly degenerate filled σ and π states. This indicates that the 14.7-eV σ-σ transition occurs near the $L-M$ axis. Band structures predict energies of this order at this point, however, they indicate that the π valence bands lie about 5 eV above the σ levels.[9,12,13]

The oscillator strength has been rearranged quite a bit from the case with q in the plane. The first doublet contains only 0.9 electrons, however, the transition at 9.9-eV contains 1.3 electrons, which causes the sum rule to increase faster between 10 and 12 eV than it does with q in the plane, when the transitions are coming from π levels. However, the transitions from the π bands into σ levels do not saturate nearly as fast, and this leads to a much slower increase at higher energies. In fact with q in the plane, the sum rule approaches 7 at 40 eV, whereas with q along c it is still less than 6. In graphite, this has been attributed to a low density of allowed transitions from occupied π bands into the lower-lying σ conduction bands,[26] which appears to be the case in h-BN also.

IV. CONCLUSIONS

The electronic properties of h-BN vary quite a bit from sample to sample. We have measured a fairly consistent intrinsic band gap of 5.9 ± 0.2 eV in three samples whose defect content varied by a factor of 4. The loss functions with q in the a-b plane are characterized by plasmons at 8.5 and 26.4 eV which are well described as collective oscillations of bound electrons. With q along the c axis, collective oscillations occur at 7.7, 11.7, and 23 eV. With q in or out of the plane, interband transitions occur at nearly the same energies with nearly the same widths. This indicates a similarity in the occupied σ and π bands not predicted by any band structure. An additional transition occurs at 9.9 eV with q along c.

ACKNOWLEDGMENTS

We would like to thank P. C. Gibbons and V. Celli for some helpful discussions. We would also to thank the other members of our group, R. D. Carson, D. E. Husk, Steven Velasquez, and E. L. Benitez, for their input. This research was supported in part by National Science Foundation (NSF) Grant No. DMR-85-15684.

[1]D. Hoffman, G. L. Doll, and P.C. Eklund, Phys. Rev. B **30**, 6051 (1984).
[2]U. Büchner, Phys. Status Solidi B **81**, 227 (1977).
[3]M. J. Rand and J. F. Roberts, J. Electrochem. Soc. **115**, 423 (1968).
[4]W. Baronian, Mater. Res. Bull. **7**, 119 (1972).
[5]M. R. Vilanove, C. R. Acad. Sci. Ser. B **271**, 1101 (1971); **272**, 1066 (1972).
[6]M. S. Nakhmanson and V. P. Smirnoff, Fiz. Tverd. Tela (Leningrad) **13**, 2309 (1972) [Sov. Phys.—Solid State B **13**, 2763 (1972)].
[7]R. Dovesi, C. Pisani, and C. Roetti, Int. J. Quantum Chem. **17**, 517 (1980).
[8]A. Zunger, A. Katzir, and A. Halperin, Phys. Rev. B **13**, 5560 (1976).
[9]John Robertson, Phys. Rev. B **29**, 2131 (1984).
[10]J. Zupan and D. Kolar, J. Phys. C **5**, 3097 (1972).
[11]Alex Zunger, J. Phys. C **7**, 76 (1974); **7**, 96 (1974).
[12]E. Doni and E. Pastori Parravicini, Nuovo Cimento B **64**, 117 (1969).
[13]A. Catellani, M. Posternak, A. Baldereschi, and A. J. Freeman, Phys. Rev. B **36**, 6105 (1987).
[14]F. Kuhn-Kuhnenfeld, D. Kirsten, and M. Maier, in *Etching Compositions and Processes,* edited by J. M. Collie (Noyes Data Corp., Park Ridge, N.J., 1982), p. 185.
[15]P. C. Gibbons, J. J. Ritsko, and S. E. Schnatterly, Rev. Sci. Instrum. **46**, 1546 (1975).
[16]J. R. Fields, Ph.D. thesis, Princeton University, 1974.
[17]Peteris Livins and S. E. Schnatterly, Phys. Rev. B **38**, 5511 (1988).
[18]R. Geick, C. H. Perry, and G. Rupprecht, Phys. Rev. **146**, 543 (1966).
[19]S. E. Schnatterly, in *Solid State Physics,* edited by H. Ehrenreich, F. Seitz, and D. Turnbull (Academic, New York, 1979), Vol. 34.
[20]H. Raether, *Springer Tracts in Modern Physics* (Springer-Verlag, Berlin, 1980), Vol. 88.
[21]F. Wooten, *Optical Constants of Solids* (Academic, New York, 1972), p. 120.
[22]E. Tegeler, N. Kosuch, G. Wiech, and A. Faessler, Phys. Status Solidi B **91**, 223 (1979).
[23]A. Mansour and S. E. Schnatterly, Phys. Rev. B **36**, 9234 (1987).
[24]J. Barth, C. Kunz, and T. M. Zimkina, Solid State Commun. **36**, 453 (1980).
[25]R. Leapan and J. Silcox, Phys. Rev. Lett. **42**, 1361 (1979); R. Leapman, P. L. Fejes, and J. Silcox, Phys. Rev. B **28**, 2361 (1983).

[26]E. Tosatti and F. Bassani, Nuovo Cimento B **65**, 161 (1970).
[27]C. H. Chen and J. Silcox, Phys. Rev. Lett. **35**, 390 (1975).
[28]J. D. Jackson, *Classical Electrodynamics* (Wiley, New York, 1975), Chap. 14.
[29]D. L. Greenaway, G. Harbeke, F. Bassani, and E. Tosatti, Phys. Rev. **178**, 134 (1969).
[30]K. Zeppenfeld, Phys. Lett. **25A**, 335 (1967).
[31]K. Zeppenfeld, thesis, Hamburg University, 1969.
[32]H. Venghaus, Phys. Status Solidi B **71**, 609 (1975).
[33]R. Mamy, J. Thomas, G. Jezequel, and J. C. Lemmonier, J. Phys. (Paris) Lett. **42**, 473 (1981).